PET Using a GRPR Antagonist ^{68}Ga-RM26 in Healthy Volunteers and Prostate Cancer Patients

Jingjing Zhang*[1–3], Gang Niu*[3], Xinrong Fan*[4], Lixin Lang[3], Guozhu Hou[1,2], Libo Chen[1,2], Huanwen Wu[5], Zhaohui Zhu[1,2], Fang Li[1,2], and Xiaoyuan Chen[3]

[1]Department of Nuclear Medicine, Peking Union Medical College (PUMC) Hospital, Chinese Academy of Medical Science & PUMC, Beijing, China; [2]Beijing Key Laboratory of Molecular Targeted Diagnosis and Therapy in Nuclear Medicine, Beijing, China; [3]Laboratory of Molecular Imaging and Nanomedicine (LOMIN), National Institute of Biomedical Imaging and Bioengineering (NIBIB), National Institutes of Health (NIH), Bethesda, Maryland; [4]Department of Urology, Peking Union Medical College (PUMC) Hospital, Chinese Academy of Medical Science & PUMC, Beijing, China; and [5]Department of Pathology, Peking Union Medical College (PUMC) Hospital, Chinese Academy of Medical Science & PUMC, Beijing, China

This study was designed to analyze the safety, biodistribution, and radiation dosimetry of a gastrin-releasing peptide receptor (GRPR) antagonist PET tracer, ^{68}Ga-RM26; to assess its clinical diagnostic value in prostate cancer patients; and to perform a direct comparison between GRPR antagonist ^{68}Ga-RM26 and agonist ^{68}Ga-BBN. **Methods:** Five healthy volunteers were enrolled to validate the safety of ^{68}Ga-RM26 and calculate dosimetry. A total of 28 patients with prostate cancer (17 newly diagnosed and 11 posttherapy) were recruited and provided written informed consent. All the cancer patients underwent PET/CT at 15–30 min after intravenous injection of 1.85 MBq (0.05 mCi) per kilogram of body weight of ^{68}Ga-RM26. Among them, 22 patients (11 newly diagnosed and 11 posttherapy) underwent ^{68}Ga-BBN PET/CT for comparison within 1 wk. ^{99m}Tc-MDP (methylene diphosphonate) bone scans were obtained within 2 wk for comparison. GRPR immunohistochemical staining of tumor samples was performed. **Results:** The administration of ^{68}Ga-M26 was well tolerated by all subjects, with no adverse symptoms being noticed or reported during the procedure and at 2-wk follow-up. The total effective dose equivalent and effective dose were 0.0912 ± 0.0140 and 0.0657 ± 0.0124 mSv/MBq, respectively. In the 17 patients with newly diagnosed prostate cancer, ^{68}Ga-RM26 PET/CT showed positive prostate-confined findings in 15 tumors with an SUV_{max} of 6.49 ± 2.37. In the 11 patients who underwent prostatectomy or brachytherapy with or without androgen deprivation therapy, ^{68}Ga-RM26 PET/CT detected 8 metastatic lymph nodes in 3 patients with an SUV_{max} of 4.28 ± 1.25 and 21 bone lesions in 8 patients with an SUV_{max} of 3.90 ± 3.07. Compared with ^{68}Ga-RM26 PET/CT, GRPR agonist ^{68}Ga-BBN PET/CT detected fewer primary lesions and lymph node metastases as well as demonstrated lower tracer accumulation. There was a significant positive correlation between SUV derived from ^{68}Ga-RM26 PET and the expression level of GRPR ($P < 0.001$). **Conclusion:** This study indicates the safety and significant efficiency of GRPR antagonist ^{68}Ga-RM26. ^{68}Ga-RM26 PET/CT would have remarkable value in detecting both primary prostate cancer and metastasis. ^{68}Ga-RM26 is also expected to be better than GRPR agonist as an imaging marker to evaluate GRPR expression in prostate cancer.

Key Words: GRPR antagonist; RM26; PET; dosimetry; prostate cancer

J Nucl Med 2018; 59:922–928
DOI: 10.2967/jnumed.117.198929

Prostate cancer has one of the highest incidence rates and is one of the most highly lethal malignant diseases in men worldwide, with roughly 758,700 new cases diagnosed per year (*1*). Accurate diagnosis and staging of prostate cancer is of utmost importance for effective therapy, especially at an early stage (*2*). Currently, the diagnosis of prostate cancer is usually triggered by elevated serum prostate-specific antigen (PSA) level, determined by anatomic imaging such as MRI, CT, or transrectal ultrasound (*3*) and confirmed with prostate biopsy (*4*). These strategies are still considered to be inadequate because PSA level can be elevated in benign conditions and increases with advancing age, and a certain portion of prostate cancer lesions might still be missed with these anatomic imaging modalities (*5*).

PET with various imaging probes has been developed to interrogate different pathways of malignant diseases including metabolism, proliferation, and abnormal receptor expression (*6*). PET radiotracers targeting prostate-specific membrane antigen (PSMA) and gastrin-releasing peptide receptor (GRPR) have shown promising results for the detection of primary and metastasized prostate cancer in early clinical studies (*7–9*).

GRPR is a member of the G protein–coupled receptor family of bombesin receptors. GRPR is overexpressed in various types of human tumors including prostate cancer, breast cancer, colorectal cancer, pancreatic cancer, small cell lung cancer, head and neck squamous cell tumors, gastric carcinoma and gastrointestinal stromal tumors, neuroblastomas, and gliomas (*10–13*). Bombesin is an amphibian homolog of mammalian gastrin-releasing peptide and its fragmental peptide BBN(7-14) has been extensively used for the development of molecular probes for the imaging of GRPR (*14*). As an agonist, BBN(7-14) showed suboptimal pharmacokinetics in vivo and would induce side effects in patients, because of its physiologic activity (*9,15*). Therefore, imaging probes based on

Received Jul. 6, 2017; revision accepted Oct. 30, 2017.
For correspondence or reprints contact either of the following:
Zhaohui Zhu, National Institutes of Health, 35A Convent Dr., GD937, Bethesda, MD 20892-3759.
E-mail: 13611093752@163.com
Xiaoyuan Chen, National Institutes of Health, 35A Convent Dr., GD937, Bethesda, MD 20892-3759.
E-mail: shawn.chen@nih.gov
*Contributed equally to this work.
Published online Nov. 9, 2017.

GRPR antagonists have been explored, and several GRPR antagonist–based PET tracers have been investigated in the clinic (*13,16,17*). Indeed, the clinical application of several such antagonists including RM2 and NeoBOMB1 showed promising potential in prostate cancer detection and staging (*16,18*).

RM26, a GRPR antagonist with high affinity, was discovered by peptide backbone modification of bombesin analogs (*19,20*). Preclinical studies confirmed that ^{68}Ga-RM26 displayed high and specific uptake in tumors and high tumor-to-background ratios (*21*). In this study, we aimed to apply GRPR antagonist PET tracer ^{68}Ga-RM26 (^{68}Ga-1,4,7-triazacyclononane-*N,N′,N″*-triacetic acid-D-Phe-Gln-Trp-Ala-Val-Gly-His-Sta-Leu-NH_2) for first-in-human studies.

MATERIALS AND METHODS

Radiopharmaceutical Preparation

NOTA-RM26 was synthesized according to the previously reported procedure with a PEG3 linker between NOTA and RM26 (*21*). The radiolabeling of NOTA-RM26 and BBN was performed in a sterile hot cell following a procedure reported previously (*10*). The radiochemical purity of the products ^{68}Ga-RM26 and ^{68}Ga-BBN was over 95%.

Subject Enrollment

This clinical study was approved by the Institutional Review Board of Peking Union Medical College Hospital, Peking Union Medical College, Chinese Academy of Medical Sciences, and all subjects gave written informed consent. This study was registered at clinicaltrials.gov (NCT03164837).

Five healthy volunteers (3 men, 2 women; age range, 32–54 y [mean age ± SD, 45.2 ± 9.5 y]; weight range, 55.0–78.0 kg [mean weight ± SD, 67.4 ± 9.2 kg]) were enrolled to validate the safety of ^{68}Ga-RM26. A total of 28 patients (age range, 57–79 y; mean age ± SD, 68.9 ± 5.86 y) were recruited, in which 17 patients were newly diagnosed by sextant core-needle biopsy without any prior therapy and 11 patients had histologically confirmed prostate cancer, underwent prostatectomy or radiation therapy or brachytherapy with or without androgen deprivation therapy, and were diagnosed as having biochemical recurrence according to the American Urological Association Prostate Guideline and American Society for Therapeutic Radiology and Oncology criteria. The demographics of the patients are listed in Supplemental Tables 1 and 2 (supplemental materials are available at http://jnm.snmjournals.org). All the 28 patients underwent ^{68}Ga-RM26 PET/CT, and 22 patients also underwent ^{68}Ga-BBN PET/CT for comparison within 1 wk. MRI or enhanced CT and MDP (methylene diphosphonate) bone scintigraphy were performed within 2 wk for comparison. All 17 primary prostate cancer patients underwent 12-core systematic randomized biopsy, and 10 of these 17 patients underwent prostatectomy with surgical pathology. Each imaging region corresponded to 2 needle prostate biopsy points, respectively. GRPR immunohistochemical staining of tumor samples against GRPR was performed and correlated with PET. The existence of malignancy in the prostate gland and lymph nodes was confirmed by histologic examination with postoperation sampling or biopsy. The examination was determined by 2 pathologists independently, with a third pathologist to reach consensus if there were any discrepancies.

Examination Procedures

For healthy volunteers, the blood pressure, pulse, respiratory frequency, and temperature were measured, and routine blood and urine tests, liver function, and renal function were examined immediately before and 24 h after the scan. In addition, any possible side effects during ^{68}Ga-RM26 PET/CT scanning and within 1 wk after the examination were collected and analyzed.

No specific subject preparation was requested on the day of ^{68}Ga-RM26 PET/CT. For the volunteers, after the whole-body low-dose CT scan, 111–148 MBq (3–4 mCi) of ^{68}Ga-RM26 were injected intravenously, followed by serial whole-body PET acquisitions. The whole body (from the top of the skull to the middle of the femur) of each volunteer was covered by 6 bed positions. The acquisition duration was 40 s/bed position at 5 and 10 min after injection and 2 min/bed position at 15, 30, 45, and 60 min after injection.

For the patients, ^{68}Ga-RM26 PET/CT scanning was performed at 15–30 min after tracer administration. For each patient, 1.85 MBq (0.05 mCi) of ^{68}Ga-RM26 per kilogram of body weight were injected intravenously. After a low-dose CT scan, whole-body PET was performed with 2 min per bed position (5–6 bed positions depending on the height of the patient). The emission data were corrected for randoms, dead time, scattering, and attenuation. The conventional reconstruction algorithm was used, and the images were zoomed with a factor of 1.2. The images were transferred to a MMWP workstation (Siemens) for analysis.

Twenty-two patients, including 11 patients with newly diagnosed prostate cancer and 11 patients with recurrent prostate cancer, underwent ^{68}Ga-BBN PET/CT for comparison within 1 wk. For each patient, 1.85 MBq (0.05 mCi) of ^{68}Ga-BBN per kilogram of body weight were injected intravenously. The imaging procedure and data analysis were the same as those for ^{68}Ga-RM26 PET/CT. The

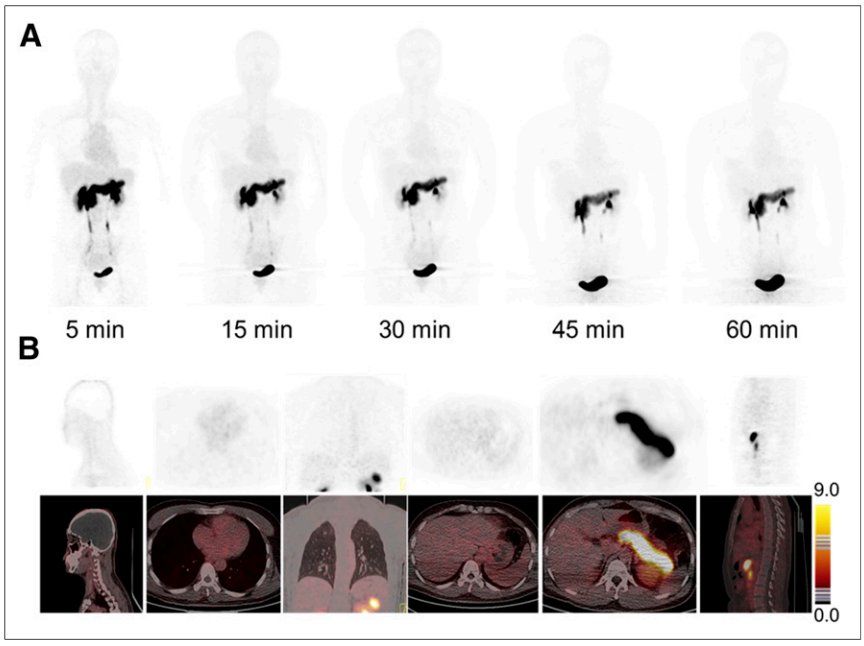

FIGURE 1. (A) Representative torso maximum-intensity-projection images of a 42-y-old female healthy volunteer at 5, 15, 30, 45, and 60 min after intravenous injection of ^{68}Ga-RM26. Main regions with prominent ^{68}Ga-RM26 uptake are pancreas, kidneys, urinary ducts, and bladder. (B) PET/CT showed tracer uptake in major organs at 30 min after intravenous administration of 129.5 MBq (3.5 mCi) of ^{68}Ga-RM26 to a 48-y-old male healthy volunteer.

contrast-enhanced CT and multiparametric MRI (Mp-MRI) were also performed.

Image Data Analysis

A Siemens MMWP workstation was used for postprocessing. Visual analysis was used to determine the general biodistribution and the temporal and intersubject stability. The volume of interest of normal organs/tissues and concerned lesions were drawn on the serial images. The radioactivity concentration and SUV in the volumes of interest were obtained through the software.

The dosimetry calculation was performed according to the European Association of Nuclear Medicine Dosimetry Guidance (*22*) and calculated using OLINDA/EXM (version 1.1; Vanderbilt University), with the procedure reported in a previous study (*10*). The void time of the bladder was set as 60 min. The absorbed doses were calculated by entering the time-integrated activity coefficient for all source organs into OLINDA/EXM for either a 73.7-kg adult man or a 56.9-kg adult woman.

Regions of interest were drawn manually on the site of lesions using a 3-dimensional ellipsoid isocontour on each image with the assistance of the corresponding CT images by 2 experienced nuclear medical physicians. The results were expressed as SUV_{mean} and SUV_{max}. Prostate MR and enhanced CT imaging were assessed by 2 experienced radiologists with the updated international prostate MR guideline protocols based on Prostate Imaging Reporting and Data system, version 2.

^{99m}Tc-MDP Bone Scintigraphy

Bone scintigraphy images were obtained using a dual-head Siemens SPECT scanner. Planar images of the whole-body skeleton were acquired in the anterior and posterior views 3 h after intravenous injection of 925 MBq (25 mCi) of ^{99m}Tc-MDP.

Immunohistochemical Staining

Representative tumor and lymph node samples were fixed with 10% neutral buffered formalin and embedded in paraffin. After blocking and washing, 5-mm-thick tissue sections were incubated with mouse antihuman polyclonal antibody against human GRPR (Ab39963; Abcam). Six fields were randomly selected from each section and observed using a light microscope (BX41; Olympus). For semiquantification of GRPR expression, 5 entire high-power fields (×40) containing clusters of malignant cells were identified randomly per slide and scored for intensity and percentage of GRPR staining expression. The procedure was repeated by 2 independent experienced examiners.

Tumor sections were scored based on the GRPR immunostaining intensity and percentage of positive tumor cells. The immunostaining intensity was graded as 0, none; 1, weak; 2, moderate; and 3, strong. The percentage of positive tumor cells was 0%–100%. And the composite score was generated by multiplying the intensity score by the percentage of positive cells.

Statistical Analysis

Statistical analysis was performed with Prism 5.0 software (GraphPad). Continuous variables were summarized as mean ± SD. The correlation between quantitative parameters was evaluated by Pearson correlation coefficient for data with normal distribution or Spearman correlation coefficient for data with skewed distribution. The Student *t* test was used to compare the SUVs of ^{68}Ga-RM26 PET and ^{68}Ga-BBN PET. All tests were 2 tailed, with the significance level at 0.05.

RESULTS

Safety and Biodistribution

No adverse events or serious adverse events occurred after ^{68}Ga-RM26 injection for all the healthy volunteers and the patients, and no obvious changes in vital signs or clinical laboratory tests were found before and after the injection of ^{68}Ga-RM26.

As shown in Figure 1, the whole-body background of ^{68}Ga-RM26 was low, which facilitated the detection of both primary and metastatic lesions. Because of endogenous GRPR expression (*23*), the pancreas showed relatively high signal intensity, with an SUV_{mean} of 20.34 ± 2.54 at 30 min after tracer injection (Supplemental Table 3). ^{68}Ga-RM26 was mainly cleared through the renal–urinary system, so bladder voiding was necessary before PET scanning. The spleen and liver showed moderate uptake, with SUVs of 1.28 ± 0.24 and 1.26 ± 0.20 at 30 min after injection, respectively. Uptake in the skeletal system, brain, lungs, mediastinum, and thorax were at background level.

Dosimetry

The estimated absorbed dose of ^{68}Ga-RM26 for each organ derived from PET images of healthy volunteers (n = 5) is shown

TABLE 1
Estimated Absorbed Dose After Intravenous Administration of ^{68}Ga-RM26

Target organ	Mean	SD
Adrenals	7.48E–03	2.71E–03
Brain	1.25E–03	4.08E–04
Breasts	4.56E–03	2.41E–03
Gallbladder wall	8.00E–03	2.67E–03
Lower large intestine wall	1.74E–02	3.64E–03
Small intestine	1.04E–02	2.84E–03
Stomach wall	7.51E–03	2.83E–03
Upper large intestine wall	9.44E–03	3.06E–03
Heart wall	5.93E–03	2.78E–03
Kidneys	3.60E–02	1.89E–03
Liver	1.59E–02	2.43E–03
Lungs	6.01E–03	1.01E–03
Muscle	7.76E–03	1.19E–03
Ovaries	2.06E–02	
Pancreas	2.25E–01	3.77E–02
Red marrow	9.15E–03	1.88E–03
Osteogenic cells	1.04E–02	4.07E–03
Skin	5.16E–03	2.17E–03
Spleen	1.93E–02	1.41E–03
Testes	1.09E–02	6.08E–04
Thymus	5.07E–03	2.60E–03
Thyroid	4.73E–03	2.42E–03
Urinary bladder wall	1.09E+00	2.25E–01
Uterus	3.55E–02	
Total body	9.98E–03	2.51E–03
Effective dose equivalent	9.12E–02	1.40E–02
Effective dose	6.57E–02	1.24E–02

Data are mSv/MBq, n = 5, 3 men and 2 women.

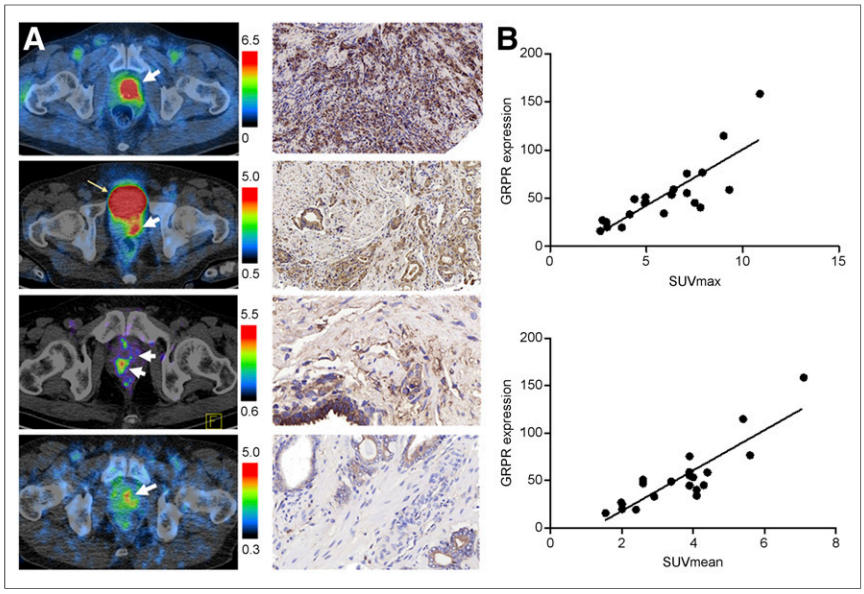

FIGURE 2. (A) Different levels of ^{68}Ga-RM26 accumulation in newly diagnosed prostate cancer and immunohistologic staining against GRPR of the biopsy samples. (B) Correlation of PET quantification and GRPR expression score in primary prostate cancer and metastases.

in Table 1. Because of the high accumulation of radioactivity in the urinary bladder, the urinary bladder wall had the highest absorbed dose of 1.09 ± 0.26 mSv/MBq. The high uptake of ^{68}Ga-RM26 in the pancreas resulted in an absorbed dose of 0.225 ± 0.038 mSv/MBq. The total effective dose equivalent and effective dose were 0.0912 ± 0.0140 and 0.0657 ± 0.0124 mSv/MBq, respectively.

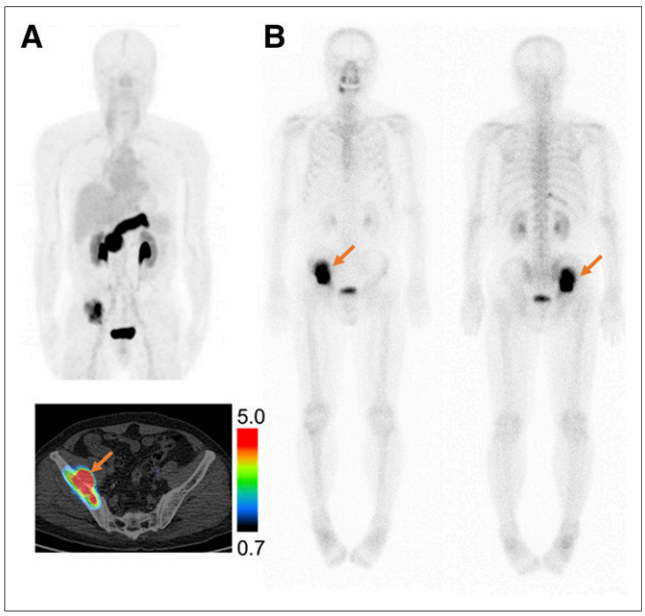

FIGURE 3. ^{68}Ga-RM26 PET/CT (A) and ^{99m}Tc-MDP bone scintigraphy (B) in a 62-y-old man with recurrent prostate cancer, who was diagnosed as having prostate cancer 4.5 y earlier and underwent radiotherapy and androgen deprivation therapy. Current PSA value was 36.0 ng/mL. ^{68}Ga-RM26 PET/CT detected bone metastasis lesion in right ilium and surrounding soft tissues.

^{68}Ga-RM26 PET/CT in Patients with Newly Diagnosed Prostate Cancer

For the 17 patients with pathologically diagnosed prostate cancer, when an SUV_{max} with a cutoff value of 2.0 and at least 1.5 times higher than the surrounding tissues was used, ^{68}Ga-RM26 PET/CT showed positive findings in 15 patients (88.2%), with an SUV_{max} of 2.71–10.9 (mean ± SD, 6.49 ± 2.37). Eleven of 17 (65%) patients had strong localized tracer accumulation in primary prostate-confined lesions, with an SUV_{max} higher than 5.0 (Supplemental Fig. 1). No significant positive correlation between SUV_{max} from ^{68}Ga-RM26 PET and Gleason score or PSA level was identified. ^{68}Ga-RM26 PET/CT also detected 19 metastatic lymph nodes in 3 patients, with an SUV_{max} of 2.47–9.2 (mean ± SD, 4.98 ± 2.15), and 21 bone metastasis lesions in 4 patients, with SUV_{max} of 1.9–13.7 (mean ± SD 5.91 ± 4.52), respectively. The immunohistochemical staining result showed positive GRPR expression in 21 of 23 samples (91.7%), including 17 samples from primary tumor needle biopsy or postoperative samples and 4 postoperative pelvic lymph node samples. There was significant positive correlation between ^{68}Ga-RM26 PET SUV and expression level of GRPR ($P < 0.001$) (Fig. 2). On the basis of the Mp-MR scanning and Prostate Imaging Reporting and Data System, version 2, criteria, 12 of 17 (70.6%) primary prostate lesions and 6 lymph nodes were detected. No additional lesions were detected by enhanced CT. In comparison to that, ^{68}Ga-RM26 PET/CT detected 15 of 17 (88.2%) primary prostate lesions in a population with an average PSA of 55.7 ± 92.0 ng/mL (Supplemental Table 1) and 9 lymph nodes in the same pelvic scanning area. ^{68}Ga-RM26 PET/CT detected more bone metastatic lesions ($n = 2$) than bone scintigraphy (Supplemental Table 1).

^{68}Ga-RM26 PET/CT in Patients with Recurrent Prostate Cancer

Eleven patients with pathologically diagnosed prostate cancer underwent prostatectomy or brachytherapy with/without androgen deprivation therapy. In these patients, ^{68}Ga-RM26 PET/CT detected 8 metastatic lymph nodes in 3 patients, with an SUV_{max} of 1.98–5.35 (mean ± SD, 4.28 ± 1.25), and 21 bone lesions in 8 patients, with an SUV_{max} of 1.51–9.77 (mean ± SD, 3.90 ± 3.07) (Fig. 3). The immunohistochemical staining revealed positive GRPR expression in 3 samples from pelvic lymph node metastasis in 1 patient. All the remaining 4 lymph nodes and 23 bone lesions were confirmed by further imaging or by response to site-directed therapies.

Comparison Between ^{68}Ga-RM26 PET/CT and ^{68}Ga-BBN PET/CT in Prostate Cancer

Among 28 patients recruited, 22 patients underwent both ^{68}Ga-RM26 and ^{68}Ga-BBN PET/CT for a direct comparison (Supplemental Tables 1 and 2; Fig. 4). ^{68}Ga-RM26 PET/CT detected 13 primary tumors, 19 lymph node lesions, and 31 bone lesions. With the same patient population, 5 primary tumors, 9 lymph nodes,

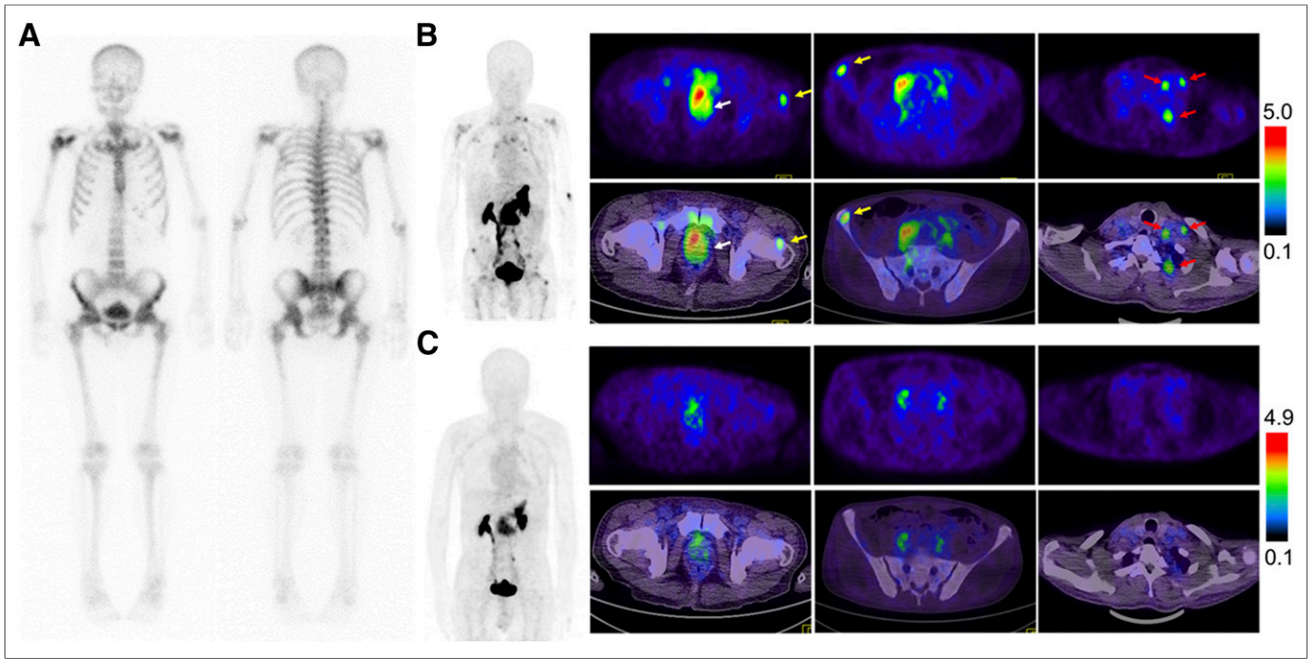

FIGURE 4. Comparison of ^{99m}Tc-MDP bone scintigraphy (A), ^{68}Ga-RM26 PET/CT (B), and ^{68}Ga-BBN PET/CT (C) in a 73-y-old man diagnosed as having prostate cancer (white arrow) with lymph node involvement (red arrow) and bone metastasis (yellow arrow) before prostatectomy. ^{68}Ga-RM26 PET/CT detected primary tumors, multiple lymph node involvement, and bone metastasis lesion, whereas those lesions did not significantly show up on ^{99m}Tc-MDP bone scintigraphy and showed extremely mild uptake on ^{68}Ga-BBN PET/CT.

and 25 bone lesions were positive on ^{68}Ga-BBN PET/CT. Moreover, SUV_{max} from ^{68}Ga-RM26 PET/CT was significantly higher than that from ^{68}Ga-BBN PET/CT in both primary lesions (2.71–9.00 [mean ± SD, 5.69 ± 1.90] vs. 1.70–4.85 [mean ± SD, 2.71 ± 1.31], $P < 0.01$) and lymph node metastases (2.23–5.90 [mean ± SD, 3.92 ± 1.20 vs. 1.30–4.30 [mean ± SD, 2.32 ± 0.95], $P < 0.01$). However, there was no significant difference of SUV_{max} in bone lesions (1.30–9.77 [mean ± SD, 4.27 ± 2.25] vs. 1.37–9.34 [mean ± SD, 4.21 ± 2.31], $P > 0.05$) (Fig. 5). Two primary tumors that were positive on ^{68}Ga-RM26 PET but negative on ^{68}Ga-BBN PET were confirmed to have moderate GRPR expression from immunohistochemical staining of the biopsy samples.

DISCUSSION

Although quite a few studies supported the idea that a GRPR antagonist is better than agonist in lesion detection, there is also reported discrepancy claiming that the agonist peptide ligand is a superior molecular imaging agent for targeting GRPR (*24*). To clarify this debate, we performed the first direct comparison of a GRPR antagonist (RM26) and agonist (BBN(7-14)) in the clinical setting.

Excretion of ^{68}Ga-RM26 is mainly through the renal–urinary tract, resulting in high radioactivity accumulation and dose exposure in the urinary bladder. With a typical 130-MBq (3.5 mCi) injected activity of ^{68}Ga-RM26, the whole-body effective dose was 8.54 mSv, which was much lower than the dose limit set by the Food and Drug Administration (*25*). All these data confirmed the safety of ^{68}Ga-RM26 for further clinical applications. However, the high exposure to the pancreas and urinary bladder needs to be considered when RM26-based endoradiotherapy is pursued.

With a large cohort of clinical samples, GRPR expression was found to be positive in around 80% of primary prostate carcinomas (*26*). Herein, ^{68}Ga-RM26 PET/CT showed positive findings in 15 of 17 primary lesions (88.2%) in patients with newly diagnosed prostate cancer, and strong localized tracer accumulation was

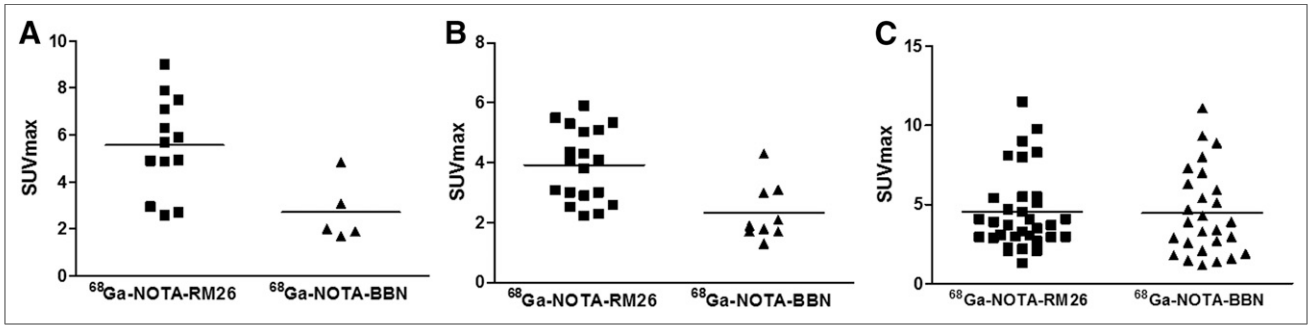

FIGURE 5. Quantitative comparison between ^{68}Ga-RM26 PET/CT and ^{68}Ga-BBN PET/CT in primary tumor (A), lymph node metastases (B), and bone metastases (C) in 22 of 28 patients who underwent both ^{68}Ga-RM26 and ^{68}Ga-BBN PET/CT.

found in 11 lesions (65%), with SUV_{max} more than 5.0. Moreover, there was a significant positive correlation between SUV from ^{68}Ga-RM26 PET and the expression level of GRPR ($P < 0.001$). However, no significant positive correlation between SUV_{max} from ^{68}Ga-RM26 PET and Gleason score was identified. In addition, there was no significant positive correlation between PSA-T or PSA-F level and SUV_{max} from ^{68}Ga-RM26 PET.

In 22 patients who underwent PET/CT using both GRPR antagonist and agonist probes, the antagonist PET identified more primary tumors with significantly higher SUV, suggesting that ^{68}Ga-RM26 antagonist tracer is potentially better than ^{68}Ga-BBN agonist tracer in lesion detection and evaluation of GRPR expression. Moreover, ^{68}Ga-RM26 PET/CT detected more lymph node metastases and bone metastases than ^{68}Ga-BBN PET/CT. RM26 showed high binding affinity for GRPR even after chelator conjugation (*27*), which is close to that of the agonist BBN (*14*). As the antagonist, RM26 showed a much lower internalization rate than BBN determined by in vitro cell experiments (*28*). We speculated that the differences in in vivo stability and pharmacokinetic profile would be the main reasons for the difference of ^{68}Ga-BBN and ^{68}Ga-RM26 in primary prostate cancer and metastasis detection.

Lesions with high receptor expression may be positively identified by both agonist and antagonist. However, lesions with low or medium receptor expression may not have high enough contrast to be visualized by the agonist. Therefore, this pilot study demonstrates that antagonist tracer ^{68}Ga-RM26 PET/CT is more valuable in prostate cancer diagnosis and staging. Moreover, the same ligand can be used as a therapeutic agent for tumor-targeted radionuclide therapy of prostate cancer after being labeled with α- or β-emitting radioisotopes (*29*). Most publications so far have favored the antagonists over agonists as imaging probes (*30*). However, controversial findings are also available (*24,31*). More strict comparison in both preclinical and clinical settings are still needed for further clarification.

The main limitations of this study are the relatively small number of patients investigated and the lack of histologic confirmation of the detected distant lymph node metastases and bone metastases. Furthermore, to avoid the interference from the high background in urinary system, the images were acquired at 15–30 min after tracer injection. Future work may consider imaging at a later time point along with furosemide to increase lesion detectability (*32*). Lastly, direct a comparison between ^{68}Ga-RM26 and other prostate cancer–targeting PET tracers such as choline and PSMA is missing (*2*). However, in previous studies, Minamimoto et al. compared PSMA and GRPR-targeted imaging in prostate cancer and found no significant differences in patients with biochemically recurrent prostate cancer (*33*). By targeting different prostate cancer–specific markers, each of these tracers may have advantages and limitations due to the heterogeneity of prostate cancer.

CONCLUSION

This study indicates the safety and efficiency of GRPR antagonist ^{68}Ga-RM26. ^{68}Ga-RM26 PET/CT would have remarkable value in detecting both primary prostate cancer and metastasis. ^{68}Ga-RM26 is also expected to be better than GRPR agonist as an imaging marker to evaluate GRPR expression in prostate cancer and other cancer types.

DISCLOSURE

This work was supported by the Intramural Research Program (IRP) of the National Institute of Biomedical Imaging and Bioengineering (NIBIB), National Institutes of Health (NIH), National Natural Science Foundation of China projects (81701742, 81671722), special fund for scientific research in the public interests of health (201402001), CAMS Major Collaborative Innovation Project (2016-I2M-1-011), Key Project on Inter Governmental International Scientific and Technological Innovation Cooperation in National Key Projects of Research and Development Plan (2016YFE0115400), PUMC Youth Fund, and the Fundamental Research Funds for the Central Universities (2017320003). No other potential conflict of interest relevant to this article was reported.

ACKNOWLEDGMENTS

All procedures performed in studies involving human participants were in accordance with the ethical standards of the institutional and/or national research committee and with the 1964 Helsinki declaration and its later amendments or comparable ethical standards.

REFERENCES

1. Torre LA, Bray F, Siegel RL, Ferlay J, Lortet-Tieulent J, Jemal A. Global cancer statistics, 2012. *CA Cancer J Clin.* 2015;65:87–108.
2. Maurer T, Eiber M, Schwaiger M, Gschwend JE. Current use of PSMA-PET in prostate cancer management. *Nat Rev Urol.* 2016;13:226–235.
3. Barentsz JO, Richenberg J, Clements R, et al. ESUR prostate MR guidelines 2012. *Eur Radiol.* 2012;22:746–757.
4. Heidenreich A, Bastian PJ, Bellmunt J, et al. EAU guidelines on prostate cancer: part 1—screening, diagnosis, and local treatment with curative intent: update 2013. *Eur Urol.* 2014;65:124–137.
5. Hoeks CM, Hambrock T, Yakar D, et al. Transition zone prostate cancer: detection and localization with 3-T multiparametric MR imaging. *Radiology.* 2013; 266:207–217.
6. Jones T, Price P. Development and experimental medicine applications of PET in oncology: a historical perspective. *Lancet Oncol.* 2012;13:e116–e125.
7. Schmuck S, Nordlohne S, von Klot CA, et al. Comparison of standard and delayed imaging to improve the detection rate of [^{68}Ga]PSMA I&T PET/CT in patients with biochemical recurrence or prostate-specific antigen persistence after primary therapy for prostate cancer. *Eur J Nucl Med Mol Imaging.* 2017;44: 960–968.
8. Cho SY, Gage KL, Mease RC, et al. Biodistribution, tumor detection, and radiation dosimetry of ^{18}F-DCFBC, a low-molecular-weight inhibitor of prostate-specific membrane antigen, in patients with metastatic prostate cancer. *J Nucl Med.* 2012;53:1883–1891.
9. Wieser G, Mansi R, Grosu AL, et al. Positron emission tomography (PET) imaging of prostate cancer with a gastrin releasing peptide receptor antagonist–from mice to men. *Theranostics.* 2014;4:412–419.
10. Zhang J, Li D, Lang L, et al. ^{68}Ga-NOTA-Aca-BBN(7-14) PET/CT in healthy volunteers and glioma patients. *J Nucl Med.* 2016;57:9–14.
11. Reubi JC, Korner M, Waser B, Mazzucchelli L, Guillou L. High expression of peptide receptors as a novel target in gastrointestinal stromal tumours. *Eur J Nucl Med Mol Imaging.* 2004;31:803–810.
12. Markwalder R, Reubi JC. Gastrin-releasing peptide receptors in the human prostate: relation to neoplastic transformation. *Cancer Res.* 1999;59:1152–1159.
13. Stoykow C, Erbes T, Maecke HR, et al. Gastrin-releasing peptide receptor imaging in breast cancer using the receptor antagonist ^{68}Ga-RM2 and PET. *Theranostics.* 2016;6:1641–1650.
14. Chen X, Park R, Hou Y, et al. microPET and autoradiographic imaging of GRP receptor expression with ^{64}Cu-DOTA-[Lys3]bombesin in human prostate adenocarcinoma xenografts. *J Nucl Med.* 2004;45:1390–1397.
15. Maina T, Bergsma H, Kulkarni HR, et al. Preclinical and first clinical experience with the gastrin-releasing peptide receptor-antagonist [^{68}Ga]SB3 and PET/CT. *Eur J Nucl Med Mol Imaging.* 2016;43:964–973.
16. Nock BA, Kaloudi A, Lymperis E, et al. Theranostic perspectives in prostate cancer with the Gastrin-releasing peptide receptor antagonist NeoBOMB1: preclinical and first clinical results. *J Nucl Med.* 2017;58:75–80.
17. Kähkönen E, Jambor I, Kemppainen J, et al. In vivo imaging of prostate cancer using [^{68}Ga]-labeled bombesin analog BAY86-7548. *Clin Cancer Res.* 2013; 19:5434–5443.

18. Wieser G, Popp I, Christian Rischke H, et al. Diagnosis of recurrent prostate cancer with PET/CT imaging using the gastrin-releasing peptide receptor antagonist ^{68}Ga-RM2: preliminary results in patients with negative or inconclusive [^{18}F]fluoroethylcholine-PET/CT. *Eur J Nucl Med Mol Imaging.* 2017;44:1463–1472.
19. Coy DH, Heinz-Erian P, Jiang NY, et al. Probing peptide backbone function in bombesin: a reduced peptide bond analogue with potent and specific receptor antagonist activity. *J Biol Chem.* 1988;263:5056–5060.
20. Mansi R, Wang X, Forrer F, et al. Development of a potent DOTA-conjugated bombesin antagonist for targeting GRPr-positive tumours. *Eur J Nucl Med Mol Imaging.* 2011;38:97–107.
21. Varasteh Z, Velikyan I, Lindeberg G, et al. Synthesis and characterization of a high-affinity NOTA-conjugated bombesin antagonist for GRPR-targeted tumor imaging. *Bioconjug Chem.* 2013;24:1144–1153.
22. Lassmann M, Chiesa C, Flux G, Bardies M, Committee ED. EANM Dosimetry Committee guidance document: good practice of clinical dosimetry reporting. *Eur J Nucl Med Mol Imaging.* 2011;38:192–200.
23. Kane MA, Kelley K, Ross SE, Portanova LB. Isolation of a gastrin releasing peptide receptor from normal rat pancreas. *Peptides.* 1991;12:207–213.
24. Nanda PK, Wienhoff BE, Rold TL, et al. Positron-emission tomography (PET) imaging agents for diagnosis of human prostate cancer: agonist vs. antagonist ligands. *In Vivo.* 2012;26:583–592.
25. Mittra ES, Goris ML, Iagaru AH, et al. Pilot pharmacokinetic and dosimetric studies of ^{18}F-FPPRGD2: a PET radiopharmaceutical agent for imaging $\alpha_v\beta_3$ integrin levels. *Radiology.* 2011;260:182–191.
26. Beer M, Montani M, Gerhardt J, et al. Profiling gastrin-releasing peptide receptor in prostate tissues: clinical implications and molecular correlates. *Prostate.* 2012;72:318–325.
27. Varasteh Z, Aberg O, Velikyan I, et al. In vitro and in vivo evaluation of a ^{18}F-labeled high affinity NOTA conjugated bombesin antagonist as a PET ligand for GRPR-targeted tumor imaging. *PLoS One.* 2013;8:e81932.
28. Varasteh Z, Mitran B, Rosenstrom U, et al. The effect of macrocyclic chelators on the targeting properties of the ^{68}Ga-labeled gastrin releasing peptide receptor antagonist PEG2-RM26. *Nucl Med Biol.* 2015;42:446–454.
29. Kabasakal L, AbuQbeitah M, Aygun A, et al. Pre-therapeutic dosimetry of normal organs and tissues of ^{177}Lu-PSMA-617 prostate-specific membrane antigen (PSMA) inhibitor in patients with castration-resistant prostate cancer. *Eur J Nucl Med Mol Imaging.* 2015;42:1976–1983.
30. Mansi R, Minamimoto R, Macke H, Iagaru AH. Bombesin-targeted PET of prostate cancer. *J Nucl Med.* 2016;57:67S–72S.
31. Yang M, Gao H, Zhou Y, et al. F-labeled GRPR agonists and antagonists: a comparative study in prostate cancer imaging. *Theranostics.* 2011;1:220–229.
32. Rischke HC, Beck T, Vach W, et al. Furosemide diminishes ^{18}F-fluoroethylcholine uptake in prostate cancer in vivo. *Eur J Nucl Med Mol Imaging.* 2014; 41:2074–2082.
33. Minamimoto R, Hancock S, Schneider B, et al. Pilot comparison of ^{68}Ga-RM2 PET and ^{68}Ga-PSMA-11 PET in patients with biochemically recurrent prostate cancer. *J Nucl Med.* 2016;57:557–562.